Sixth International Conference on Durability of Concrete Structures **Paper Number PSE20**
18 - 20 July 2018
University of Leeds, Leeds, West Yorkshire, LS2 9JT, United Kingdom

Drying Shrinkage of Hardened Cement Paste and Its Relationship to the Microstructure

X. Wang, C. Wan, X. Zhang and H. Chen
College of Materials Science and Engineering, Chongqing University, China

ABSTRACT

The aim of the present study is to relate microstructure to the drying shrinkage of hardened cement paste. Three microstructural features, calcium silicate hydrate(C-S-H), calcium hydroxide(CH) and pore structure were studied. A new method to determine the C-S-H content of hardened cement paste is presented. Drying shrinkage behavior of cement pastes were investigated by drying specimens through successive steps of RH 100% to 7% RH and re-saturating the specimens. The total shrinkage of cement paste after drying to 7% RH and irreversible shrinkage were decreased with the increasing amount of C-S-H and CH. Prolonged curing resulted in a paste with finer pore structure and more weight loss when dried in lower humidity. For a certain paste, the same amount of weight loss induced less liner shrinkage in the 54-23% RH range than in the 100-54% RH range. The total shrinkage of cement paste after drying to 7% RH and irreversible shrinkage decreases with increasing amount of C-S-H and CH. The formation of C-S-H increase the resistance of cement paste to shrinkage rather than enhance drying shrinkage by providing more gel pores and empty of which would bring large stress on the solid skeleton.

Keywords: hardened cement paste; drying shrinkage; calcium silicate hydrate; calcium hydroxide; pore structure

1.0 INTRODUCTION AND STRATEGY

Drying shrinkage is a characteristic property of hardened cement paste and also closely related with the durability of its corresponding concrete, for example, the drying shrinkage induced cracks can make concrete more permeable and easy to suffer chemical attack etc. Hardened cement paste is a highly porous material with a large specific surface area, primarily due to the porous microstructure of the main hydration product, $CaO–SiO_2–H_2O$ (C-S-H) (Wittmann, 1973; Thomas, Jennings and Allen, 1999). Large quantities of water vapor are adsorbed on the internal surface of the hydration products (Setzer and Wittmann, 1974). The volume of hardened cement paste is sensitive to its moisture content (Juenger and Jennings, 2002). When exposed to environmental humidity, which is less than 100% RH, a saturated paste begins to lose water and shrink. The shrinkage on first drying is partly irreversible.

An approach towards a better understanding of the mechanism of drying shrinkage would be to study the relationship between microstructure even nanostructure and drying shrinkage of hardened cement paste. In the present study, the strategy was to vary the microstructure and relate the changes to the shrinkage behavior. Variation of the microstructure of cement paste was obtained by varying the curing time.

Calcium hydroxide (CH), C-S-H, and pore structure are chosen as the microstructural features for analysis in this study. Calcium hydroxide is believed to play a role in limiting the amount of shrinkage that occurs when a cement paste is dried (Mehta and Monteiro, 2006). Most of the shrinkage occurs in the C-S-H, the formation of C-S-H could increase drying shrinkage by increasing the level of deformation occurring within the paste, or reduce shrinkage by developing a rigid network of hydration product capable of resisting shrinkage. Furthermore, since drying process involves removal of water from pores which in turn creates substantial stresses and causes shrinkage (Hansen, 1987), the characterization of pore structure is important.

Solid state ^{29}Si MAS NMR, thermal analysis, MIP, and nitrogen sorption were used for microstructure analysis and the drying shrinkage of cement paste was determined from equilibrium drying experiments which was first proposed by Roper (Roper, 1965). Tests of drying shrinkage were generally conducted by directly subjecting samples to the ultimate RH. However, according to the classic experimental results of Roper, cement paste undergoes a series of different drying shrinkage mechanisms as the paste is equilibrated at successively lower relative humidity (Roper, 1965; Jennings, Thomas and Gevrenov, 2007). Thus, a more useful approach is to conduct stepwise drying, taking care to reach equilibrium at each RH level. Therefore, drying shrinkage could be studied in different RH ranges.

2.0 EXPERIMENTS

Cement pastes were prepared by hand mixing a ASTM Type I cement (Table 1) at W/C ratio of 0.4 with de-ionized water for 5 minutes. Samples were cast in polystyrene vials (27 mm diameter, 50 mm height) and sealed in air-tight containers in a 24 ˚C water bath. After the first 24 h, samples were demoulded and cured at room temperature (24 ± 3 °C) in an air-tight container filled with lime-saturated water for ages of 7, 28, 56 and 180 days. After the specified curing time, samples were removed from the lime water and prepared for tests.

Table 1. Chemical analysis of ASTM Type I Portland cement

Mineral composition	Weight percent (%)	Chemical Composition	Weight percent (%)
C_3S	48.26	SiO_2	21.84
C_2S	26.23	Al_2O_3	4.96
C_3A	7.21	CaO	64.97
C_4AF	10.64	Fe_2O_3	3.50
		MgO	1.90
		SO_3	0.77
		Loss of ignition (%)	0.65

The equilibrium drying experiments were conducted after the method proposed by Roper (Roper, 1965) and Jennings (Jennings, Thomas and Gevrenov, 2007). Thin (0.80mm) discs were sliced using a water-lubricated diamond precision saw. Initially saturated discs were progressively dried step-by-step via enclosing them over saturated salt solutions with different equilibrium relative humidity in sealed desiccators. The desiccators were filled with nitrogen gas to prevent carbonation. The successive steps of RH were 84%, 74%, 54%, 23%, 7% and the temperature was maintained at 24 ± 3 °C. At regular intervals the discs were weighed and the length was measured using a micrometre. Only when the length and weight stabilized at one RH was the discs moved to the desiccators containing the next-level RH. Irreversible drying shrinkage was then determined by re-saturating the specimens step by step and the last step was placing specimens in lime-water.

Before measuring pore structure, samples were ground to particle sizes in the range of 600 to 1180 μm and then freeze-dried. The pore structure was measured using a nitrogen surface area analyzer (Micromeritics ASAP 2020). Porosities and pore structure were calculated by the Barret, Joyner and Hallenda (BJH) method on the adsorption isotherm.

The quantity of calcium hydroxide in the pastes was calculated by thermogravimetric analysis (TGA) method using a TG-DSC analyser (NETZSCH STA 449C). Samples were freshly crushed and ground into powder under carbonation free condition, then were heated to 1000 °C at 20°C/min, under a constant flow of nitrogen.

3.0 DETERMINATION OF C-S-H CONTENT

In the present study, the C-S-H content was determined from a combination results of thermogravimetric analysis and single pulse ^{29}Si solid state MAS NMR. The strategy was to calculate the percentage of SiO_2 reacted in the raw materials via ^{29}Si NMR analysis.

Single pulse ^{29}Si solid state MAS NMR spectra were acquired using a Bruker AVANCE III 400MHz spectrometer (operating frequency of 79.49 MHz for ^{29}Si). Samples were packed into 7 mm ZrO_2 rotors and spun at 6 kHz. The spectra were acquired over 10000 scans using a pulse recycle delay of 3 s, a pulse width 4.5 μs, and an acquisition time 10.29 ms.

Deconvolution of the spectra provides quantitative information on the fractions of Si present in different tetrahedral environments, Q_n, where n denotes the connectivity of the silicate tetrahedron: thus Q_0 represents isolated tetrahedra in the anhydrous paste (at around -71 ppm); Q_1 represents chain-end group tetrahedral (at round -79 ppm), Q_2 represents middle groups where both adjacent tetrahedral are occupied by silicon tetrahedral (at round -83 ppm), Q_3 represents branching sites and Q_4 cross-linking sites in a three dimensional framework (Cong and Kirkpatrick, 1996; Love, Richardson and Brough, 2007; Girão, Richardson and Porteneuve, 2007; He and Hu, 2007). Thus $\alpha = I(Q_1+Q_2+Q_3+Q_4)/ I(Q_0+Q_1+Q_2+Q_3+Q_4)$, where α denotes the percentage of Si reacted. The percentage of SiO_2 reacted equals the percentage of Si reacted.

In thermogravimetric analysis, the weight of hydrated cement paste after firing to 1000 °C, W_{1000}, represents the weight of the raw cement used. Thus, $W(SiO_2) = 0.2184 * W_{1000}$, where $W(SiO_2)$ denotes the weight of SiO_2 (SiO_2 makes up 21.84% of the original cement as shown in Table 1). And $Wr(SiO_2) = \alpha * W(SiO_2)$, where $Wr(SiO_2)$ denotes the weight of SiO_2 reacted.

The stoichiometry of C-S-H is assumed to be $C_{3.4}S_2H_3$ (Mindess and Young, 1981; Olson and Jennings, 2001). According to the law of conservation of mass, that is, the quantity of the SiO_2 reacted equals to that of the SiO_2 in the hydration products, $W(C\text{-}S\text{-}H) * M(S_2) / M(C_{3.4}S_2H_3) = Wr(SiO_2)$, where M denotes molar mass, $M(S_2) / M(C_{3.4}S_2H_3)$ denotes the SiO_2 content in $C_{3.4}S_2H_3$, $M(S_2) / M(C_{3.4}S_2H_3) = 0.3293$. Thus, $W(C\text{-}S\text{-}H) = Wr(SiO_2) * M(C_{3.4}S_2H_3) / M(S_2) = 0.6632 * \alpha * W_{1000}$, where W(C-S-H) denotes the weight of C-S-H. Therefore, the C-S-H content can be calculated

using the equation: %C-S-H = W(C-S-H) / W_{paste} = 0.6632*α*W_{1000} / W_{paste}, where W_{paste} denotes the weight of dried paste at 105℃.

4.0 RESULTS AND DISCUSSION

4.1. Characterization of Microstructure

CH and C-S-H

Typical TG- DSC results were presented in Fig. 1, and corresponds to the results obtained for cement paste hydrated for 28 days. The first endothermic peak of DSC curve is attributed to the de-hydroxylation of C-S-H phase, corresponding to the mass loss on the TG profile around 200℃ (Neto, Cincotto and Repette, 2008; Alarcon-Ruiza, Platret, Massieu and Ehrlacher, 2005; Esteves, 2011). The second major peak of DSC curve is also endothermic and mainly corresponds to the decomposition of calcium hydroxide between 400-500℃ or so (Neto, Cincotto and Repette, 2008; Alarcon-Ruiza, Platret, Massieu and Ehrlacher, 2005; Esteves, 2011), the exact temperature interval can be clearly identified by DSC curve as shown in Fig. 1. No representative peak was found at DSC curve around 800℃. The quantity of calcium hydroxide in the pastes determined from the thermogravimetric curves are given in Table 2 (as percentage of paste dried at 105℃). As expected, calcium hydroxide contents of samples increase with the curing time.

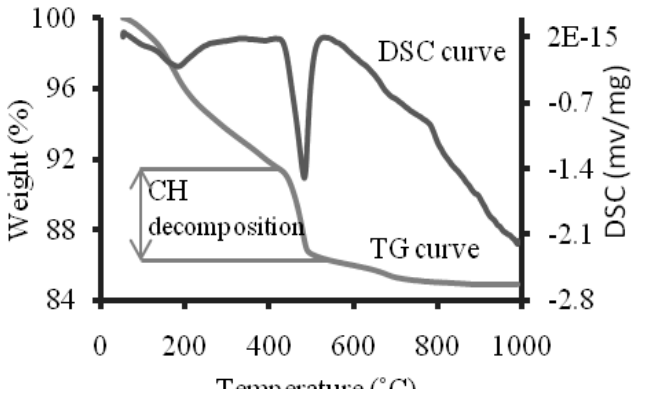

Fig. 1. Thermal analysis data for the 28-day-old cement paste

Typical single-pulse ^{29}Si solid state NMR results were presented in Fig. 2, and corresponds to the results obtained for cement paste hydrated for 28 days, the same as in Fig. 1. In the studied system, no Q_3 and Q_4 were found. The results of the deconvolution of spectra are given in Table 2. As shown, C-S-H contents of cement pastes and Q_2 contents of C-S-H increase with the curing time,

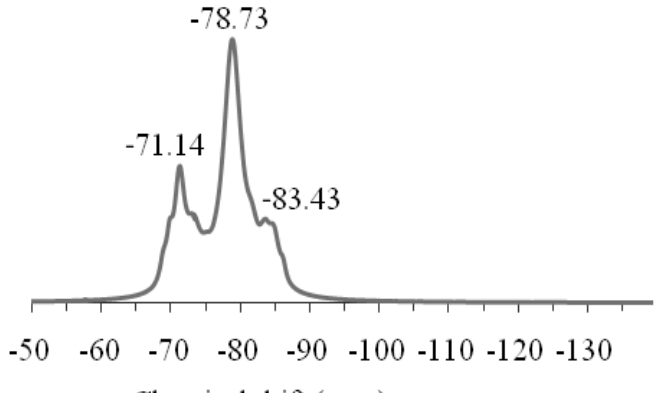

Fig. 2. Single-pulse ^{29}Si solid state NMR spectra for the 28-day-old cement paste

Pore structure of C-S-H

In this study, nitrogen adsorption gives information about pores in the diameter range of 1.7-50 nm, which include small capillaries and gel pores that are associated with the C-S-H product (Mehta and Monteiro, 2006; Taylor, 1997).

As shown in *Fig*. 4, pores in this range are generally characterized by two classes: pores located around 30 nm and around a few nanometers, respectively. Pore size distribution for cement pastes with different curing times are displayed in Fig. 5, and the evolution of average pore diameter with curing time is shown in Fig. 6. Generally, prolonged curing increased the volume of pores around a few nanometers and resulted in a finer pore structure.

Table 2. Results from thermal analysis, ^{29}Si NMR spectra and calculation described in section 3.

age	% CH	% Q_0	%Q_1	%Q_2	% SiO_2 reacted	W_{1000}	W_{paste}	% C-S-H
7 days	15.43	38.36	58.38	3.36	61.64	8.7390	10.1585	35.17
28 days	17.70	28.30	65.35	6.35	71.70	9.0855	10.6988	40.38
56 days	17.86	24.36	63.17	12.48	75.65	8.5651	10.2888	41.74
180 days	20.58	8.24	68.17	23.59	91.76	8.3601	10.4880	48.51

%CH = calcium hydroxide as % of paste weight dried at 105 ℃. %C-S-H = calcium silicate hydrate as % of paste weight dried at 105 ℃.

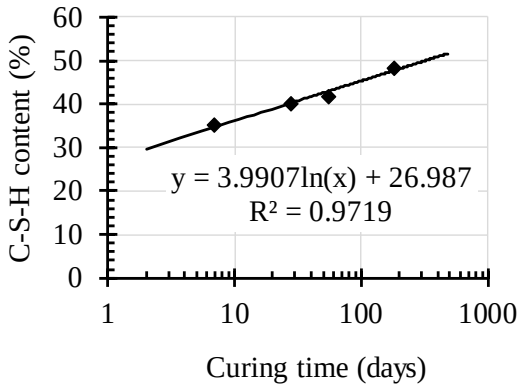

Fig. 3. C-S-H content versus curing time of hydrated cement paste

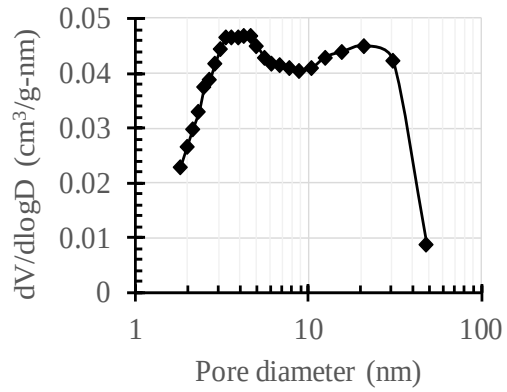

Fig. 4. Pore size distribution for the 180-day-old cement paste as measured by nitrogen adsorption

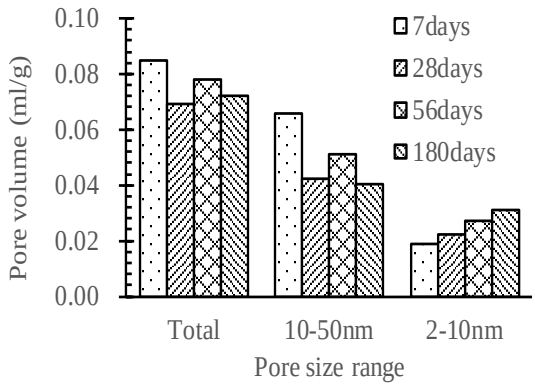

Fig. 5. Pore size distribution for cement paste with different curing time

4.2. Drying Shrinkage

The curves shown in Figs. 7a and 7b illustrate drying shrinkage and weight loss versus time during the equilibrium drying and re-saturating process. The data shown are for the 28-day-old cement paste.

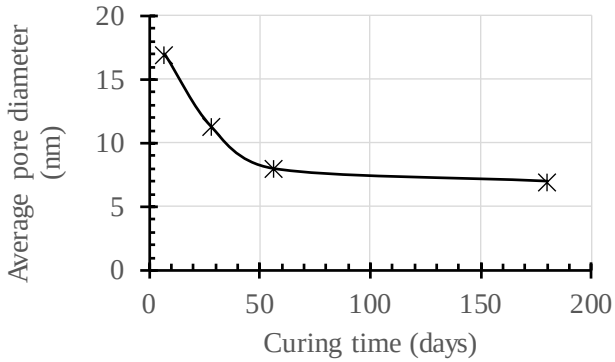

Fig. 6. Average pore diameter for cement pastes with different curing time

The curves are typical for the systems investigated and each curve is the average of the results obtained from two companion specimens. As is shown, there is a continuous increase in shrinkage and weight loss as RH decreases. After re-saturating, weight loss can be almost fully regained while a large portion of the drying shrinkage is irreversible. There was a significant hysteresis between the weight loss and weight regaining at each RH range and a large portion of the weight loss was regained after re-immersing in the lime-water. The case was the same for shrinkage.

Shrinkage and weight loss results for cement paste of different curing time are summarized in Table 3, where total drying shrinkage is the equilibrium shrinkage value after drying to 7% RH, irreversible shrinkage is the shrinkage value after re-saturating in lime-water, and reversible shrinkage is the difference between the two. The calculation method of weight loss is similar to that of drying shrinkage.

4.3. Relationship Between Drying Shrinkage and Microstructure

Shrinkage resisting phase and drying shrinkage

In the 100 - 54% RH range, shrinkage at an earlier age (7 days) is relatively large, but at later ages, these values are lower. It is suggested that the main driving force of shrinkage in this range is associated with capillary tension (Taylor, 1997). On the one hand, according to the weight loss data in Table 3, less volume of pores is dried to empty with age which means fewer menisci was formed, with less water having high capillary tension, resulting in lower stress and subsequently lower shrinkage strains. On the other hand, as indicated by the ^{29}Si NMR spectra data, extended curing not only increased the C-S-H content in hydrated cement paste but also increased the polymerization of C-S-H according to the % Q_2

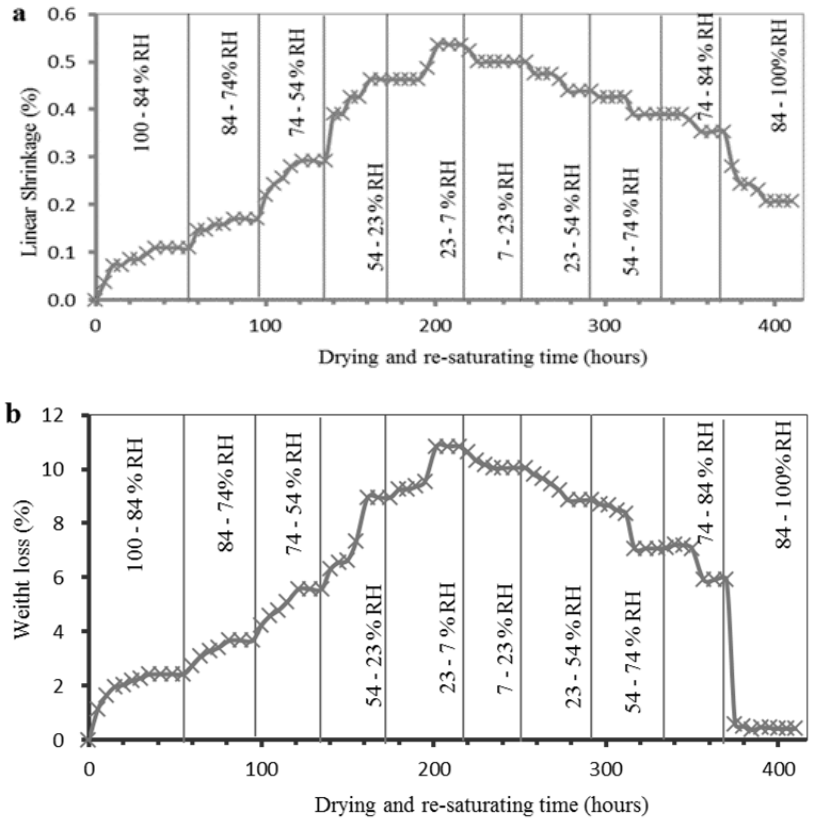

Fig. 7. (a) drying shrinkage of the 28-day-old hardened cement paste under equilibrium drying and re-saturating, (b) weight loss of the 28-day-old hardened cement paste under equilibrium drying and re-saturating

Table 3. Drying shrinkage and weight loss results for cement pastes of different curing time

	Shrinkage (% in length change)/ Weight loss (% in mass change)					
	Total	100- 54% RH	54-23% RH	23-7% RH	Irreversible	Reversible
7 days	0.566/13.17	0.359/8.52	0.120/3.01	0.087/1.64	0.290/-	0.276/-
28 days	0.536/10.87	0.292/5.60	0.171/3.60	0.073/1.67	0.205/-	0.329/-
56 days	0.509/11.98	0.266/5.49	0.158/4.99	0.085/1.50	0.157/-	0.352/-
180 days	0.459/11.84	0.264/5.44	0.122/5.09	0.073/1.29	0.133/-	0.326/-

Irreversible weight loss was not calculated because weight loss can be almost fully regained.

data in Table 2. C-S-H grows more and stronger over time, developing a rigid network of hydration product inserted with more CH as the restraining phase according to the %CH data in Table 2. Thus, the resulting cement paste is stiffer and possesses a higher modulus, which would shrink less even under the same stress.

In the 54 - 23% RH range, shrinkage is likely due to the empty of smaller pores (e.g., < 10 nm), which are associated with the main hydration product, i.e., C-S-H. The volume of smaller pores increases over time as indicated by the nitrogen porosity data. Weight loss data in Table 3 also indicates that the volume of pores emptied in this range increases with increasing age of paste, which should result in higher shrinkage strains. However, shrinkage in this range increases from 7 days to 28 days, and then decreases with age. Again, a reasonable explanation should be that C-S-H grows more and stronger over time, resulting in a stiffer paste with a higher modulus, and shrink less even under higher stress.

In the 23 - 7% RH range, weight loss and shrinkage show very relatively tiny decrease trend with curing time. Shrinkage in this range are likely due to the empty of the smallest pores which cannot be detected by the nitrogen porosity analysis (Mindess and Young, 1981; Juenger and Jennings, 2001).

On the whole, in the 100 - 7% RH range, the total and irreversible shrinkage decrease with curing time, that is, with the increasing content of C-S-H and CH.

From the shrinkage analysis above, it could be concluded that CH and C-S-H appears to increase the resistance of hydrated cement paste to drying shrinkage and that the shrinkage of cement paste depends mainly on its resistance to deformation.

Table 4. Ratio of weight loss and relationship between weight loss and shrinkage in each RH range

Curing time	Ratio of weight loss (%)/ Shrinkage per weight loss(*10^{-2})		
	100- 54% RH	54-23% RH	23-7% RH
7 days	64.69/0.0421	22.86/0.0399	12.45/0.0530
28 days	51.52/0.0523	33.11/0.0475	15.36/0.0437
56 days	45.82/0.0484	41.65/0.0322	12.52/0.0567
180 days	46.02/0.0485	43.06/0.0240	10.91/0.0566

Pore structure and drying shrinkage

Table 4 summarizes the ratio of weight loss occurred in each RH range for pastes with different curing time. For the 7-day-old paste, 64.69% of the weight loss occurred in the 100 - 54%RH range. For older pastes, the ratio of weight loss in this range decreases and more ratio of weight loss occurred below 54% RH. Data from nitrogen sorption as indicated in *Fig*. 4 and 6 shows that older pastes have a finer pore structure.

For the 7-day-old paste, 1% of weight loss induces 0.0421% of linear shrinkage in the 100 – 54% RH range. In the 54 – 23% RH range, 1% of weight loss induces only 0.0399% of linear shrinkage. Detailed results for pastes of different curing time are summarized in Table 4. It could be identified that for a certain paste, the same amount of weight loss induced less linear shrinkage in the 54 - 23% RH range than in the 100 - 54% RH range. A reasonable explanation could be that the modulus of cement paste increases after drying, and thus will shrink less even under higher stress. There is evidence in literature that drying caused an increase in polymerization (Bentur, Berger, Lawrence Jr., Milestone, Mindess and Young, 1979), which would result in a stiffer paste. Besides, the mechanical behaviour of cement paste could be described in the framework of porous media, and the bulk modulus of paste would increase with the loss of water (Ghabezloo, Sulem, Guédon, Martineau and Saint-Marc, 2008; Vlahinić, Jennings and Thomas, 2009).

5.0 CONCLUSIONS

C-S-H grows more and stronger over time, resulting in a stiffer and denser paste structure. The total shrinkage of cement paste after drying to 7% RH and irreversible shrinkage decreases with increasing amount of C-S-H and CH. The formation of C-S-H increase the resistance of cement paste to shrinkage rather than enhance drying shrinkage by providing more gel pores and empty of which would bring large stress on the solid skeleton. Detailed study of drying shrinkage and weight loss of cement pastes in different RH ranges indicates that prolonged curing time resulted in a paste with a finer pore structure and more weight loss when dried in lower humidity and that for a certain paste, the same amount of weight loss induced less linear shrinkage in the 54 - 23% RH range than in the 100-54% RH range. This would probably be a reason why the presence of more gel pores doesn't bring larger drying shrinkage.

Acknowledgement

We gratefully acknowledge the financial support provided by the National Natural Science Foundation of China, Grant No. 51172292, named as Insight into the Micro- and Nano- Scale Mechanism of Drying Shrinkage of Hardened Cement Paste.

References

Alarcon-Ruiza, L., Platret, G., Massieu, E., Ehrlacher, A., 2005. The use of thermal analysis in assessing the effect of temperature on a cement paste. Cement and Concrete Research, 35(3):609–613.

Bentur, A., Berger, R.L., Lawrence Jr., F.V., Milestone, N.B., Mindess, S., Young, J.F.,1979. Creep and drying shrinkage of calcium silicate pastes: III. A hypothesis of irreversible strains. Cement and Concrete Research, 9(1):83–95.

Cong, X., Kirkpatrick, R.J., 1996. ^{29}Si MAS NMR study of the structure of calcium silicate hydrate. Advanced Cement Based Materials, 3(3-4):144-156.

Esteves, L.P., 2011. On the hydration of water-entrained cement–silica systems: Combined SEM, XRD and thermal analysis in cement pastes. Thermochimica Acta, 518(1-2):27–35.

Ghabezloo, S., Sulem, J., Guédon, S., Martineau, F., Saint-Marc, J., 2008. Poromechanical behavior of hardened cement paste under isotropic loading. Cement and Concrete Research, 38(12):1424–1437.

Girão, A.V., Richardson, I.G., Porteneuve, C.B., 2007. Composition, morphology and nanostructure of C–S–H in white Portland cement pastes hydrated at 55 °C. Cement and Concrete Research, 37(12):1571–1582.

Hansen, W., 1987. Drying shrinkage mechanisms in Portland cement paste. Journal of the American Ceramic Society, 70(5):323-328.

He, Y., Hu, S., 2007. Application of ^{29}Si nuclear magnetic resonance (NMR) in research of cement chemistry. Journal of Materials Science & Engineering, 25(1):147-153. (in Chinese)

Jennings, H.M., Thomas, J.J., Gevrenov, J.S., 2007. A multi-technique investigation of the nanoporosity of cement paste. Cement and Concrete Research, 37(3):329–336.

Juenger, M.C.G., Jennings, H.M., 2001. The use of nitrogen adsorption to assess the microstructure of cement paste. Cement and Concrete Research, 31(6):883-892.

Juenger, M.C.G., Jennings, H.M., 2002. Examining the relationship between the microstructure of calcium silicate hydrate and drying shrinkage of cement pastes. Cement and Concrete Research, 32(2):289–296.

Love, C.A., Richardson, I.G., Brough, A.R., 2007. Composition and structure of C–S–H in white Portland cement–20% metakaolin pastes hydrated at 25 °C. Cement and Concrete Research, 37(2):109–117.

Mehta, P.K., Monteiro, P.J.M., 2006. Concrete: Microstructure, properties, and materials (3rd ed.). New York, NY: McGraw-Hill, ISBN 0-07-146289-9.

Mindess, S., Young, J.F., 1981. Concrete, Englewood Cliffs, N.J.:Prentice-Hall, ISBN 0-13-167106-5.

Neto, A.A.M., Cincotto, M.A., Repette, W., 2008. Drying and autogenous shrinkage of pastes and mortars with activated slag cement. Cement and Concrete Research, 38(4):565–574.

Olson, R.A., Jennings, H.M., 2001. Estimation of C-S-H content in a blended cement paste using water adsorption. Cement and Concrete Research, 31(3):351-356.

Roper, H., 1965. Dimensional change and water sorption studies of cement paste, Proceedings of the symposium on structure of Portland cement paste and concrete, Washington, D.C.:Highway Research Board, Division of Engineering, National Research Council, National Academy of Sciences-National Academy of Engineering. 74–83.

Setzer, M.J., Wittmann, F.H., 1974. Surface energy and mechanical behavior of hardened cement paste. Applied Physics, 3(5):403-409.

Taylor, H.F.W., 1997. Cement Chemistry (2nd ed.), London: Thomas Telford, ISBN 0-7277-2592-0.

Thomas, J.J., Jennings, H.M., Allen, A.J., 1999. The surface area of hardened cement paste as measured by various techniques. Concrete Science and Engineering, 1:45–64.

Vlahinić, I., Jennings, H.M., Thomas, J.J., 2009. A constitutive model for drying of a partially saturated porous material. Mechanics of Materials, 41(3):319–328.

Wittmann, F.H., 1973. Observation of an electromechanical effect of hardened cement paste. Cement and Concrete Research, 3(5):601–605.